ISSN 1392–1320 MATERIALS SCIENCE (MEDŽIAGOTYRA). Vol. 30, No. 2. 2024

Chloride Ion Penetration Resistance of Reactive Powder Concrete with Mineral Admixtures

Xinmin YU [1], Hongji ZHANG [2], Dehong WANG [2], Yanzhong JU [2], Mengxin KANG [2]*, Yidan MA [2]

[1] *State GRID Fujian Economic Research Institute, No. 68 Road Chayuan, Fuzhou 350013, Fujian Province, China*
[2] *School of Civil Engineering and Architecture, Northeast Electric Power University, No. 169 Road Changchun, Jilin, 132012, China*

http://doi.org/10.5755/j02.ms.34962

Received 29 August 2023; accepted 20 November 2023

This study employed the rapid chloride ion penetration test and the salt spray erosion method to examine electric flux changes in mineral-admixed reactive powder concrete (RPC). Variations in the chloride ion content and diffusion coefficient under different erosion durations and depths were also investigated. The impact of mineral admixtures on the chloride penetration resistance was explored. Notably, after mixing fly ash (FA) and granulated blast furnace slag (GGBS), the electric flux values of RPC of each group were significantly reduced, and the electric flux values of RPC of the mixed group were significantly lower than those of the single mixed group and the reference group, in which the electric flux of FA10G10 was reduced by 85.2 % compared to the control group; at the same erosion cycle and depth, the chloride ion content and diffusion coefficient of the mixed group were significantly lower than the control group. It shows that the reasonable compounding of mineral admixtures can better exert the "superposition effect", improve the compactness inside the matrix, and effectively reduce the chloride ion penetration rate. Considering comprehensively, the FA10G10 group has the best chloride penetration ion resistance effect.

Keywords: reactive powder concrete, mineral admixture, chloride ion penetration, electric flux, chloride diffusion coefficient.

1. INTRODUCTION

Reinforced concrete structures are widely used in construction projects due to their excellent mechanical properties. However, because of the complexity of the environment in which reinforced concrete is located, various durability problems will occur during its use [1 – 7]. Especially in the saline and coastal areas of China, reinforced concrete structures and infrastructure are often threatened by chloride ion erosion [8 – 11]. Chloride ions can penetrate the interior of reinforced concrete structures and cause corrosion of the reinforcing steel, resulting in expansion and cracking of the concrete, which significantly weakens the mechanical properties and durability of concrete structures [12 – 16]. Chloride ions penetrate concrete in two forms: partly by chemical reaction with C3A and C4AF to form Friedel's salt, or by adsorption on calcium silicate hydrate (C-S-H), both of which are known as bound chloride ions [17]. The other part is in the form of free chloride ions that exist inside the concrete and gradually penetrate the surface of the steel reinforcement, eventually leading to corrosion of the reinforcement [18 – 20]. The penetration process of chloride ions in concrete is a complex diffusion process, the rate of which is influenced by a variety of factors, such as the pore structure of concrete, water-cement ratio, hydration products, temperature, etc. [17, 21 – 24].

Reactive Powder Concrete (RPC) is an advanced concrete material with superior properties that offer significant advantages in resisting chloride ion penetration [25-29]. RPC has a very dense microstructure and excellent impermeability [30], making it difficult for chloride ions to penetrate the concrete. Its high strength and low W/C ratio design reduce the number and size of concrete pores and harmful pores, thus limiting the penetration channels for chloride ions [31]. The use of mineral admixtures such as fly ash (FA), silica fume (SF), and granulated blast furnace slag (GGBS) to replace part of the cement in RPC can improve the matrix densification of RPC and effectively hinder the diffusion of free chloride ions. In addition, mineral dopants can undergo a secondary hydration reaction with calcium hydroxide to form C-S-H gels, which increases the binding capacity of the matrix for chloride ions [32 – 34]. Currently, there have been studies on the effect of incorporating mineral admixtures in concrete on the performance of chloride penetration resistance, Wang [35] delved into the chloride ion permeability attributes of concrete modified with FA and SF under freeze-thaw circumstances. The findings demonstrated the concrete's electrical flux could be effectively mitigated by an optimal combination of FA and SF. Notably, SF showcased a more pronounced efficacy in augmenting the concrete's chloride ion permeability. Otieno [36] explored the ramifications of varying w/b ratios and substituting slag in terms of concrete's resistance against chloride ion penetration by employing distinct chemical compositions of slag. The study unearthed a noteworthy enhancement in the concrete's ability to fend off chloride ion intrusion. This enhancement was closely associated with diminished w/b ratios and increased slag

* Corresponding author. Tel.: +86-43264806481; fax: +86-43264806429.
E-mail: *20122416@neepu.edu.cn* (M. Kang)

substitution levels. However, there is a lack of research on the chloride penetration resistance of mineral admixtures incorporated in RPC.

Therefore, the variation rule of RPC's anti-chlorine ion penetration performance under different mineral admixture substitutions was investigated by using the electric flux method and the salt spray erosion method in this study. The effects of mineral dopants on the pore structure and chloride ion binding properties of RPC were explored, and the effects of these factors on the permeability to anti-chlorine ions were further investigated. By thoroughly studying the chloride ion penetration mechanism and the interaction of mineral admixtures, it is possible to gain a deeper understanding of the effect of mineral admixtures on RPC, which in turn improves the durability of concrete structures and provides a more reliable theoretical basis for the application of RPC in highly erosive environments.

2. MATERIALS AND METHODS

2.1. Raw material and mixture proportions

Cement, SF, FA, GGBS, quartz sand, basalt fibers, water reducer, and water are the raw materials for RPC. The cement is P·O42.5 Portland cement; silica fume has a particle size of less than 2 μm, a specific surface area of 19 m^2/g, and silica content of 82.2 %; FA is Class I fly ash with a particle size of less than 29 μm; the GGBS is S95 grade granulated blast furnace slag powder; quartz sand including coarse, medium and fine three grain sizes, the coarse sand grain size of 10 – 20 mesh, the medium sand grain size of 20 – 40 mesh, the fine sand grain size of 10 – 20 mesh; water reducing agent for the polycarboxylic acid system of high-performance water reducing agent, the water reduction rate of 46 %; basalt fibers for the short-cut basalt fibers, fiber length of 12 mm, the aspect ratio of 1000, modulus of elasticity for the 80 – 110 GPa. Specific ratios are shown in Table 1.

2.2. Methods for characterization of chloride ion penetration resistance

2.2.1. Rapid chloride ion penetration test

The sample was cut and machined to the required size for the test. Paraffin wax was melted and evenly applied to the cylindrical side ring surfaces, checked for correctness, and then moved into the vacuum water retainer. Subsequently, the prepared specimens were mounted into the test tank and clamped, and the data were recorded every 30 min until the end of 6 h of energization, which can be used to derive the diffusion of chloride ions in the RPC, and then to evaluate the resistance to chloride ion permeation of the RPC under different ratios. Rapid chloride ion penetration test refers to ASTM C 1202 [37] and literature [38].

2.2.2. Salt spray corrosion method

The salt spray corrosion test specimen is a cube specimen with a side length of 100 mm, the specimen is dried after 28 d of maintenance, and put into the salt spray test chamber for the corrosion cycle, as shown in Fig. 1 a.

a b

Fig. 1. Experimental equipment: a – KW-ST-90 salt spray test chamber; b – JY-20 quick measuring instrument

Each cycle time is 24 h, in which the warming process is 0.5 h, the salt spray is carried out for 8 h at 35 ℃, and then it is dried in an oven at 55 ℃ for 15.5 h. The salt spray erosion solution is adopted with a concentration of 5 % sodium chloride solution. After 30 d, 60 d, and 90 d of erosion cycles, the specimens were removed for drying. Subsequently, the specimens were split into two halves and the powder was drilled layer by layer from 0 – 5 mm, 5 – 10 mm, 10 – 15 mm, and 15 – 20 mm from the exposed surface of the specimens. Each layer was selected from a different position, and the samples were ground to be fine enough, then sieved through a 0.63 mm mesh sieve, and then tested by using a JY-20 type chlorine ion content rapid tester for each group of samples. This evaluation process is repeated thrice per group to derive an average value, as illustrated in Fig. 1 b.

Quantify the concentrations of chloride ions at distinct depths within the specimen, facilitating comparative analysis of data variations across each group and depth. Furthermore, assess the diffusion coefficient's magnitude, determined by fitting Fick's second law, to draw inferences about chloride ion resistance. the surface chloride ion concentrations can be inferred from the equation $y = a - b \times c^x$. The chloride ion content at depths of 5 – 10 mm was calculated by substituting into the formula, which is illustrated in Eq. 1:

$$c(x,t) = c_0 + \left[1 - erf\left(\frac{x}{2\sqrt{Dt}}\right)\right](c_z - c_0), \quad (1)$$

where *erf* is the error function, $erf(u) = \frac{2}{\sqrt{\pi}}\int_0^u e^{-t^2} dt$; c_z represents RPC surface chloride ion concentration; c_0 represents RPC internal chloride ion concentration; c_x represents RPC chloride ion concentration at depth x mm; x is the depth from the surface; t is the chloride ion diffusion time.

3. RESULTS AND DISCUSSION

3.1. Electric flux

Fig. 2 shows the current values and their variation curves for each group of RPCs at different times. It can be observed that as the energization time increases, the current values of each group also increase gradually. Within 60 minutes of energization, the fluctuation of the current value is more obvious and then tends to stabilize.

Table 1. Mixture proportions of mineral admixture RPC

Number	The amount of each material per cubic meter /kg·m^{-3}							
	Cement	SF	FA	GGBS	Sand	Basalt fibre	Water reducer	Water
FA0G0	803.95	200.99	–	–	1,306.83	5.5	6.03	177.09
FA0G30	562.77	200.99	–	241.19	1,306.83	5.5	6.03	177.09
FA30G0	562.77	200.99	241.19	–	1,306.83	5.5	6.03	177.09
FA10G10	643.16	200.99	80.40	80.40	1,306.83	5.5	6.03	177.09
FA30G10	482.37	200.99	241.19	80.40	1,306.83	5.5	6.03	177.09
FA10G30	482.37	200.99	80.40	241.19	1,306.83	5.5	6.03	177.09

The current value of RPC in the control group was significantly higher than in other groups, and the growth rate was faster. After 360 minutes of energization, the current value of the control group RPC reaches the maximum value of 1.35 MA, while the current value of each group of mineral admixture RPC is significantly lower than the control group, especially the current value of the mixed group decreases more significantly. Among them, the FA10G10 has the best performance, with a current value of only 0.51 MA after 360 min of energization.

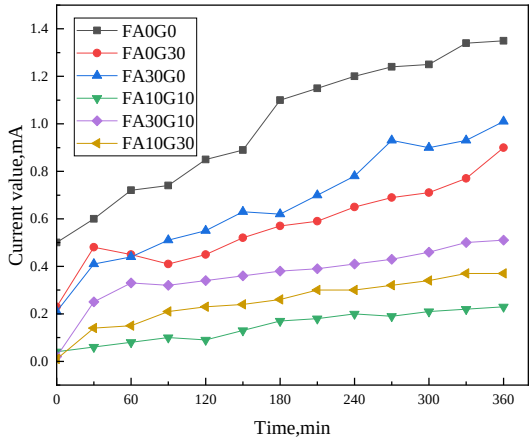

Fig. 2. Changes in current value of mineral admixtures RPC

Fig. 3 shows the comparison of the electric flux of RPC at different substitutions. It can be observed that after the single-mixed of FA and GGBS instead of cement, the electric flux of RPC decreases significantly, and the values of the electric flux of FA0G30 and FA30G0 are 11.867C and 13.833C, respectively, which are 42.4 % and 32.8 % lower than those of the control group, respectively. This is because the addition of GGBS and FA promotes the secondary hydration reaction of cement, produces dense and stable C-S-H gel, fills the pores and microcracks, and makes the concrete more dense internally [39]. It is also observed that the value of the electrical flux of single-mixed GGBS group is lower than that of single-mixed FA group, this result is in agreement with previous studies [40, 41], where the hydration reactivity of GGBS was higher than that of FA, and FA had lower early activity and slower secondary hydration reaction, resulting in a slightly higher electrical flux than that of single-mixed GGBS.

The converted flux of the FA10G10 is 3.054C, which is 85.2 % and 25.7 % less than that of the control group and the single-mixed GGBS group, respectively. This indicates that the mixed group greatly fills the pores and cracks due to the "superposition effect" of different mineral admixtures, which significantly reduces the electric flux [9]. Overall, the FA10G10 performed the best due to the better secondary hydration reaction of the mineral admixtures in this group, which significantly improved the overall bonding of the matrix slurry. In addition, due to the reasonable compounding to enhance the densification of the matrix, effectively reducing the initial defective holes, thus reducing the electric flux. The 6 h electric fluxes of RPC single-mixed groups are less than 15C, and the electric fluxes of the mixed groups are less than 10C, which shows the excellent resistance to chlorine penetration of the mineral admixtures RPC.

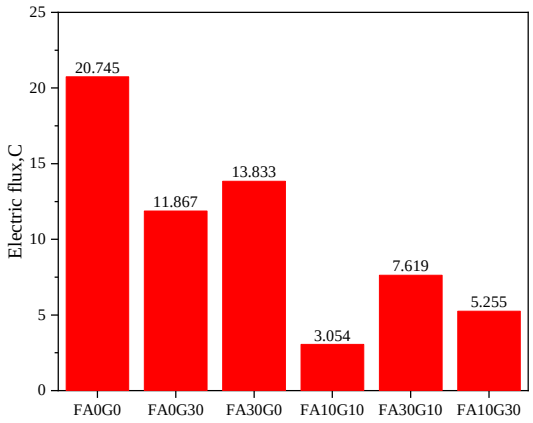

Fig. 3. RPC electric flux comparison

From the test results, it can be seen that the electric flux and the average current value into a positive correlation linear, through the test data, can be fitted to derive the relationship between the value of the electric flux and the average current value of the relationship between the equation and the correlation is better ($R^2 = 0.999$), the accuracy is high, the relationship obtained by the fitting of the equation as shown in Eq. 2, as shown in Fig. 4.

$$y = 0.09805 + 20.64665x\,, \tag{2}$$

where x is the average current, y is the electric flux.

3.2. Chloride ion diffusion coefficient

To further investigate the effect of mineral admixtures on the resistance of RPC to chloride penetration, the salt spray corrosion tests were performed under different corrosion cycles, and the measured chloride ion content under different salt spray corrosion cycles and different depths are shown in Fig. 5. The chloride content in the concretes decreases rapidly and stabilizes as the depth of measurement increases [42]. In the case of fixing the RPC

in the same group and depth, the chloride ion content keeps increasing with the increase of the erosion cycle. The chloride content of RPC in the same depth of the mixed group is smaller than that of the reference group, which indicates that the "superposition effect" played by the mixing of FA and GGBS effectively improves the resistance of RPC to chloride penetration. The FA30G10 mixture displays diminished resistance against the penetration of chloride ions.

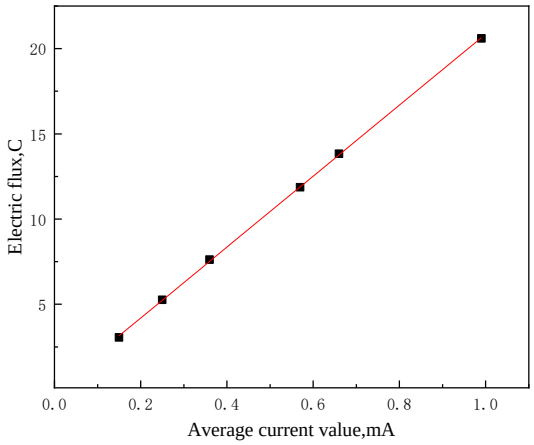

Fig. 4. Fitting line of electric flux and average current value

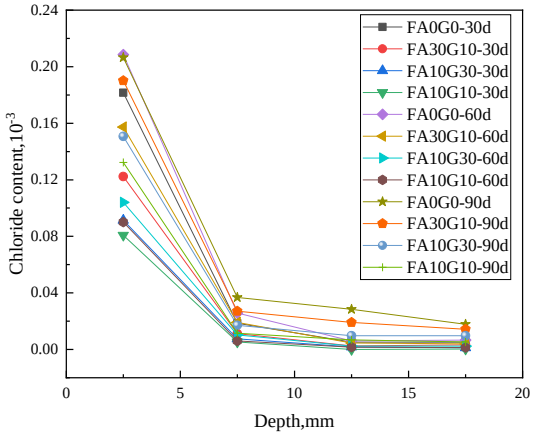

Fig. 5. Chloride contents under different salt spray corrosion cycles

The findings of Boga [43] indicate that an excessive inclusion of FA can impede the hydration reaction of a fraction of the FA, thereby resulting in an augmentation of concrete permeability. In the case of FA10G10, the variation of chloride ion content in different measurement depths was small, which showed the best chloride penetration resistance effect.

The values of the chloride diffusion coefficients and the curves of diffusion coefficients with time for each group under different erosion cycles are shown in Fig. 6. The diffusion coefficients of chloride ions decreased gradually with erosion. In addition to increasing the densification of concrete, researchers generally agree that the incorporation of FA and GGBS has a physicochemical binding effect on chloride ions [44], and the content of bound chloride ions increases gradually with the change of erosion time, and the Friedel's salt generated by the chemical reaction can fill the pore space, which can effectively impede the penetration process of chloride ions and significantly reduce the diffusion coefficient. It was observed that a larger amount of FA substitution resulted in a smaller decrease in the late diffusion coefficient, while a larger amount of GGBS substitution resulted in a larger decrease in the late diffusion coefficient, which was due to the difference in the time of participation in the hydration reaction between FA and GGBS[45 – 47].

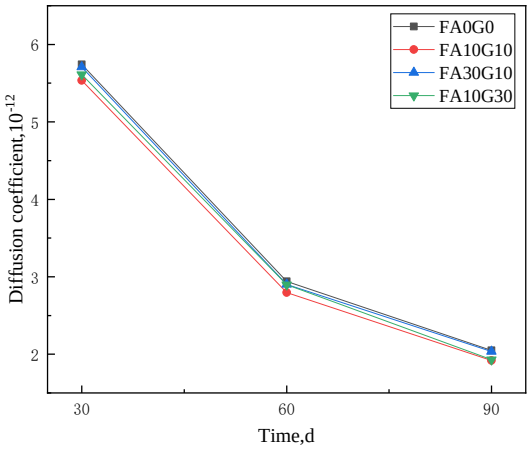

Fig. 6. The relationship between chloride diffusion coefficient and time

The diffusion coefficient of the FA10G10 was the smallest and had the slowest rate of decrease, which indicated that it had the best resistance to chloride erosion.

4. CONCLUSIONS

Through the electric flux experiments and salt spray erosion experiments, the effects of different FA and GGBS mixing methods on the anti-chlorine ion permeation performance of RPC were investigated to provide more reliable theoretical support for the application of RPC in complex erosion environments. The principal findings of this study can be summarized as follows:

1. The addition of FA and GGBS filled the pores of RPC and improved the densification of the matrix. Compared with the control group, the flux values of FA0G30 and FA30G0 in the single-mixed group were reduced by 42.4 % and 32.8 %, respectively; the flux values of the mixed group were lower than those of the single-mixed group and the control group, with the lowest flux value of 3.054C for FA10G10.
2. At the same depth, all three mixing groups had lower chloride ion levels than the control group. The higher chloride ion content was caused by the fact that some FAs in FA30G10 did not participate in the hydration reaction. And FA10G10 fully utilized the "superposition effect" and showed the best anti-chlorine ion penetration effect.
3. The addition of FA and GGBS significantly reduced the chloride diffusion coefficient. However, due to the different hydration reaction times of GGBS and FA, different substitution amounts would result in different reductions of the chloride diffusion coefficients at the later stage. A reasonable mixing method will effectively improve the chlorine ion penetration resistance of RPC.

Acknowledgments

The authors gratefully acknowledge the National Natural Science Foundation of China (Grant No. 51878128).

REFERENCES

1. **Dousti, A., Shekarchi, M., Alizadeh, R., Taheri-Motlagh, A.** Binding of Externally Supplied Chlorides in Micro Silica Concrete Under Field Exposure Conditions *Cement and Concrete Composites* 33 (10) 2011: pp. 1071 – 1079. https://doi.org/10.1016/j.cemconcomp.2011.08.002
2. **Dang, V.H., François, R.** Influence of Long-Term Corrosion in Chloride Environment on Mechanical Behaviour of RC Beam *Engineering Structures* 48 2013: pp. 558 – 568. https://doi.org/10.1016/j.engstruct.2012.09.021
3. **Qu, F., Li, W., Dong, W., Tam, V.W.Y., Yu, T.** Durability Deterioration of Concrete Under Marine Environment from Material to Structure: A Critical Review *Journal of Building Engineering* 35 2021: pp. 102074. https://doi.org/10.1016/j.jobe.2020.102074
4. **Qian, R., Li, Q., Fu, C., Zhang, Y., Wang, Y., Jin, X.** Atmospheric Chloride-Induced Corrosion of Steel-Reinforced Concrete Beam Exposed to Real Marine-Environment for 7 Years *Ocean Engineering* 286 2023: pp. 115675. https://doi.org/10.1016/j.oceaneng.2023.115675
5. **Shao, W., Wang, Y., Shi, D.** Corrosion-Fatigue Life Prediction of Reinforced Concrete Square Piles in Marine Environments *Engineering Failure Analysis* 138 2022: pp. 106324. https://doi.org/10.1016/j.engfailanal.2022.106324
6. **Jaffer, S.J., Hansson, C.M.** The Influence of Cracks on Chl oride-Induced Corrosion of Steel in Ordinary Portland Ceme nt and High Performance Concretes Subjected to Different L oading Conditions *Corrosion Science* 50 (12) 2008: pp. 3343 – 3355. https://doi.org/10.1016/j.corsci.2008.09.018
7. **Zheng, Y., Zheng, S.S., Yang, L., Dong, L.G., Ruan, S., Ming, M.** Experimental Study on the Seismic Behavior of Corroded Reinforced Concrete Walls in An Artificial Climate Corrosion Environment *Engineering Structures* 252 2022: pp. 113469. https://doi.org/10.1016/j.engstruct.2021.113469
8. **Shi, X., Xie, N., Fortune, K., Gong, J.** Durability of Steel Reinforced Concrete in Chloride Environments: An Overview *Construction and Building Materials* 30 2012: pp. 125 – 138. https://doi.org/ 10.1016/j.conbuildmat.2011.12.038
9. **Wang, D., Ma, Y., Kang, M., Ju, Y., Zeng, C.** Durability of Reactive Powder Concrete Containing Mineral Admixtures in Seawater Erosion Environment *Construction and Building Materials* 306 2021: pp. 124863. https://doi.org/10.1016/j.conbuildmat.2021.124863
10. **Wang, J., Niu, D., Wang, Y., Wang, B.** Durability Performance of Brine-Exposed Shotcrete in Salt Lake Environment *Construction and Building Materials* 188 2018: pp. 520 – 536. https://doi.org/10.1016/j.conbuildmat.2018.08.139
11. **Francois, R., Maso, J.C.** Effect of Damage in Reinforced Concrete on Carbonation or Chloride Penetration *Cement and Concrete Research* 18 (6) 1988: pp. 961 – 970. https://doi.org/10.1016/0008-8846(88)90033-6
12. **Arya, C., Buenfeld, N.R., Newman, J.B.** Factors Influencing Chloride-Binding in Concrete *Cement Concrete Research* 20 (2) 1990: pp. 291 – 300. https://doi.org/10.1016/0008-8846(90)90083-A
13. **Ju, Y., Shen, T., Wang, D.** Bonding Behavior between Reactive Powder Concrete and Normal Strength Concrete *Construction and Building Materials* 242 2020: pp. 118024. https://doi.org/10.1016/j.conbuildmat.2020.118024
14. **Nguyen, Q.D., Castel, A.** Long-term Durability of Underground Reinforced Concrete Pipes in Natural Chloride and Carbonation Environments *Construction and Building Materials* 394 2023: pp. 132230. https://doi.org/10.1016/j.conbuildmat.2023.132230
15. **Poupard, O., L'Hostis, V., Catinaud, S., Petre-Lazar, I.** Corrosion Damage Diagnosis of A Reinforced Concrete Beam after 40 Years Natural Exposure in Marine Environment *Cement and Concrete Research* 36 (3) 2006: pp. 504 – 520. https://doi.org/10.1016/j.cemconres.2005.11.004
16. **Song, C., Jiang, C., Gu, X.L., Zhang, Q., Zhang, W.P.** Calibration Analysis of Chloride Binding Capacity for Cement-Based Materials Under Various Exposure Conditions *Construction and Building Materials* 314 (Part A) 2022: pp. 125588. https://doi.org/10.1016/j.conbuildmat.2021.125588
17. **Page, C.L., Short, N.R., El Tarras, A.** Diffusion of Chloride Ions in Hardened Cement Pastes *Cement and Concrete Research* 11 (3) 1981: pp. 395 – 406. https://doi.org/10.1016/0008-8846(81)90111-3
18. **Chatterji, S.** Mechanism of the $CaCl_2$ Attack on Portland Cement Concrete *Cement and Concrete Research* 8 (4) 1978: pp. 461 – 467. https://doi.org/10.1016/0008-8846(78)90026-1
19. **Xu, J., Li, F.** A Meso-Scale Model for Analyzing the Chloride Diffusion of Concrete Subjected to External Stress *Construction and Building Materials* 130 2017: pp. 11 – 21. https://doi.org/10.1016/j.conbuildmat.2016.11.054
20. **Lin, G., Liu, Y., Xiang, Z.** Numerical Modeling for Predicting Service Life of Reinforced Concrete Structures Exposed to Chloride Environments *Cement and Concrete Composites* 32 (8) 2010: pp. 571 – 579. https://doi.org/10.1016/j.cemconcomp.2010.07.012
21. **Li, L-y., Easterbrook, D., Xia, J., Jin, W.L.** Numerical Simulation of Chloride Penetration in Concrete in Rapid Chloride Migration Tests *Cement and Concrete Composites* 63 2015: pp. 113 – 121. https://doi.org/10.1016/j.cemconcomp.2015.09.004
22. **Tian, Y., Zhang, G., Ye, H., Zeng, Q., Zhang, Z., Tian, Z.** Corrosion of Steel Rebar in Concrete Induced by Chloride Ions Under Natural Environments *Construction and Building Materials* 369 2023: pp. 130504. https://doi.org/10.1016/j.conbuildmat.2023.130504
23. **Wang, D., Han, L., Kang, M., Wan, M., Ju, Y.** Influence of Corrosion on the Bond Performance of Reinforcements and Basalt Fibre High Strength Concrete *Case Studies in Construction Materials* 17 2022: pp. e01394. https://doi.org/10.1016/j.cscm.2022.e01394
24. **Mohammed, T.U., Hamada, H.** Relationship between Free Chloride and Total Chloride Contents in Concrete *Cement and Concrete Research* 33 (9) 2003: pp. 1487 – 1490. https://doi.org/10.1016/S0008-8846(03)00065-6

25. **Bahmani, H., Mostofinejad, D.** Microstructure of Ultra-High-Performance Concrete (UHPC)-A Review Study *Journal of Building Engineering* 50 2022: pp. 104118. https://doi.org/10.1016/j.jobe.2022.104118
26. **Wang, D., Zhao, J., Ju, Y., Shen, H., Li, X.** Behavior of Beam-Column Joints with High Performance Fiber-Reinforced Concrete under Cyclic Loading *Structures* 44 2022: pp. 171 – 185. https://doi.org/10.1016/j.istruc.2022.07.090
27. **De Larrard, F., Sedran, T.** Mixture-Proportioning of High-Performance Concrete *Cement and Concrete Research* 32 (11) 2002: pp. 1699 – 1704. https://doi.org/10.1016/S0008-8846(02)00861-X
28. **De Larrard, F.** Ultrafine Particles for the Making of Very High Strength Concretes *Cement and Concrete Research* 19 (2) 1989: pp. 161 – 172. https://doi.org/10.1016/0008-8846(89)90079-3
29. **Wang, D., Ju, Y., Shen, H., Xu, L.** Mechanical Properties of High Performance Concrete Reinforced with Basalt Fiber and Polypropylene Fiber *Construction and Building Materials* 197 2019: pp. 464 – 473. https://doi.org/10.1016/j.conbuildmat.2018.11.181
30. **Ju, Y., Zhao, J., Wang, D., Song, Y.** Experimental Study on Flexural Behaviour of Reinforced Reactive Powder Concrete Pole *Construction and Building Materials* 312 2021: pp. 125399. https://doi.org/10.1016/j.conbuildmat.2021.125399
31. **Shi, C., Wu, Z., Xiao, J., Wang, D., Huang, Z., Fang, Z.** A Review on Ultra High Performance Concrete: Part I. Raw Materials and Mixture Design *Construction and Building Materials* 101 2015: pp. 741 – 751. https://doi.org/10.1016/j.conbuildmat.2015.10.088
32. **Boddy, A., Bentz, E., Thomas, M.D.A., Hooton, R.D.** An Overview and Sensitivity Study of a Multimechanistic Chloride Transport Model *Cement and Concrete Research* 29 (6) 1999: pp. 827 – 837. https://doi.org/10.1016/S0008-8846(99)00045-9
33. **Lv, X., Yang, L., Li, J., Wang, F.** Roles of Fly Ash, Granulated Blast-Furnace Slag, and Silica Fume in Long-Term Resistance to External Sulfate Attacks at Atmospheric Temperature *Cement and Concrete Composites* 133 2022: pp. 104696. https://doi.org/10.1016/j.cemconcomp.2022.104696
34. **Yazıcı, H., Yardımcı, M.Y., Yiğiter, H., Aydın, S., Türkel, S.** Mechanical Properties of Reactive Powder Concrete Containing High Volumes of Ground Granulated Blast Furnace Slag *Cement and Concrete Composites* 32 (8) 2010: pp. 639 – 648. https://doi.org/10.1016/j.cemconcomp.2010.07.005
35. **Wang, D., Zhou, X., Fu, B., Zhang, L.** Chloride Ion Penetration Resistance of Concrete Containing Fly Ash and Silica Fume Against Combined Freezing-Thawing and Chloride Attack *Construction and Building Materials* 169 2018: pp. 740 – 747. https://doi.org/10.1016/j.conbuildmat.2018.03.038
36. **Otieno, M., Beushausen, H., Alexander, M.** Effect of Chemical Composition of Slag on Chloride Penetration Resistance of Concrete *Cement and Concrete Composites* 46 2014: pp. 56 – 64. https://doi.org/10.1016/j.cemconcomp.2013.11.003
37. Standard Test Method for Electrical Indication of Concrete's Ability to Resist Chloride Ion Penetration: ASTM International; 2012. https://doi.org/10.1520/C1202-10
38. **Wang, J., Dong, H.** PVA Fiber-Reinforced Ultrafine Fly Ash Concrete: Engineering Properties, Resistance to Chloride Ion Penetration, and Microstructure *Journal of Building Engineering* 66 2023: pp. 105858. https://doi.org/10.1016/j.jobe.2023.105858
39. **Nayak, D.K., Abhilash, P.P., Singh, R., Kumar, R., Kumar, V.** Fly Ash for Sustainable Construction: A Review of Fly Ash Concrete and its Beneficial Use Case Studies *Cleaner Materials* 6 2022: pp. 100143. https://doi.org/10.1016/j.clema.2022.100143
40. **Shi, H.S., Xu, B.W., Zhou, X.C.** Influence of Mineral Admixtures on Compressive Strength, Gas Permeability and Carbonation of High Performance Concrete *Construction and Building Materials* 23 (5) 2009: pp. 1980 – 1985. https://doi.org/10.1016/j.conbuildmat.2008.08.021
41. **Leng, F., Feng, N., Lu, X.** An Experimental Study on the Properties of Resistance to Diffusion of Chloride Ions of Fly Ash and Blast Furnace Slag Concrete *Cement and Concrete Research* 30 (6) 2000: pp. 989 – 992. https://doi.org/10.1016/S0008-8846(00)00250-7
42. **Sabet, F.A., Libre, N.A., Shekarchi, M.** Mechanical and Durability Properties of Self Consolidating High Performance Concrete Incorporating Natural Zeolite, Silica Fume and Fly Ash *Construction and Building Materials* 44 2013: pp. 175 – 184. https://doi.org/10.1016/j.conbuildmat.2013.02.069
43. **Boğa, A.R., Topçu, İ.B.** Influence of Fly Ash on Corrosion Resistance and Chloride Ion Permeability of Concrete *Construction and Building Materials* 31 2012: pp. 258 – 264. https://doi.org/10.1016/j.conbuildmat.2011.12.106
44. **Thomas, M.D.A., Hooton, R.D., Scott, A., Zibara, H.** The Effect of Supplementary Cementitious Materials on Chloride Binding in Hardened Cement Paste *Cement and Concrete Research* 42 (1) 2012: pp. 1 – 7. https://doi.org/10.1016/j.cemconres.2011.01.001
45. **Han, C., Shen, W., Ji, X., Wang, Z., Ding, Q., Xu, G.** Behavior of High Performance Concrete Pastes with Different Mineral Admixtures in Simulated Seawater Environment *Construction and Building Materials* 187 2018: pp. 426 – 438. https://doi.org/10.1016/j.conbuildmat.2018.07.196
46. **Rangarao, M.L.S., Pradhan, B.** Effect of Chloride and Blend of Chloride And Sulphate Salts on Workability, Early Strength and Microstructure of FA-GGBS Geopolymer Concrete *Materials Today: Proceedings* 65 2022: pp. 3907 – 3911. https://doi.org/10.1016/j.matpr.2022.07.196
47. **Alexander, A.E., Shashikala, A.P.** Studies on the Microstructure and Durability Characteristics of Ambient Cured FA-GGBS Based Geopolymer Mortar *Construction and Building Materials* 347 2022: pp. 128538. https://doi.org/10.1016/j.conbuildmat.2022.128538

.